

# Degradability of Poly(Lactic Acid)-Containing Nanoparticles: Enzymatic Access through a Cross-Linked Shell Barrier

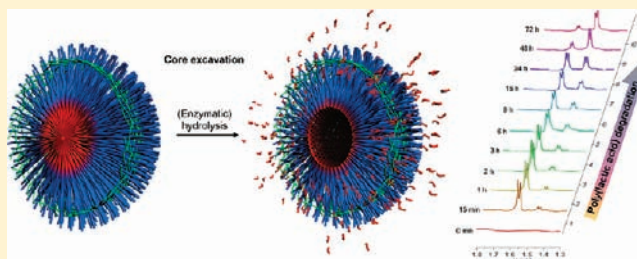
Sandani Samarajeewa,<sup>†</sup> Ritu Shrestha,<sup>†</sup> Yali Li,<sup>‡,§</sup> and Karen L. Wooley<sup>\*,†</sup>

<sup>†</sup>Departments of Chemistry and Chemical Engineering, Texas A&M University, College Station, Texas 77842, United States

<sup>‡</sup>Departments of Chemistry and Radiology, Washington University, St. Louis, Missouri 63130, United States

**S** Supporting Information

**ABSTRACT:** Comparative studies of bulk samples of hydrolytically degradable poly(lactic acid) (PLA) vs core–shell block copolymer micelles having PLA cores revealed remarkable acceleration in the proteinase K enzymatic hydrolysis of the nanoparticulate forms and demonstrated that even with amidation-based shell cross-linking the core domain remained accessible. Kinetic analyses by <sup>1</sup>H NMR spectroscopy showed less than 20% lactic acid released from enzymatically catalyzed hydrolysis of poly(L-lactic acid) in bulk, whereas ca. 70% of the core degraded within 48 h for block copolymer micelles of poly(*N*-(acryloyloxy)succinimide-*co*-polymer-*N*-acryloylmorpholine)-*block*-poly(L-lactic acid) (P(NAS-*co*-NAM)-*b*-PLLA), with only a slight reduction to ca. 50% for the shell cross-linked derivatives. Rigorous characterization measurements by NMR spectroscopy, fluorescence spectroscopy, dynamic light scattering, atomic force microscopy, and transmission electron microscopy were employed to confirm core excavation. These studies provide important fundamental understanding of the effects of nanoscopic dimensions on protein–polymer interactions and polymer degradability, which will guide the development of these degradable nanoconstructs to reach their potential for controlled release of therapeutics and biological clearance.



## INTRODUCTION

There has been a growing interest in employing degradable materials for applications in biomedical settings, due to their reduced toxicity and ability to clear through biological systems. Biodegradable polymers were first developed for sutures in the 1960s,<sup>1</sup> and this technology was later adopted for controlled drug delivery purposes, followed by clinical translations in the 1980s.<sup>2</sup> After one of the earliest works on drug-loaded degradable microparticles based on poly(lactic acid) (PLA)-peptide drug formulations, reported by DuPont in 1973,<sup>3</sup> the utilization of biodegradable materials for sustained release has emerged immensely.

Therapeutics can be loaded into polymeric nanoconstructs, and the release of these encapsulated guest molecules can then be triggered by external stimuli such as changes in pH,<sup>4,5</sup> light,<sup>6</sup> and temperature.<sup>7</sup> However, for rapid and effective clinical translation, it is imperative that these nanostructures are comprised of biocompatible materials,<sup>8</sup> which can package therapeutics, gate their release, and provide efficient delivery. Complex polymeric nanostructures with core–shell morphologies that constitute degradable polyesters in the core domain have shown great potential as vehicles for delivery of active therapeutics.<sup>9–20</sup>

Our group has a long-standing interest in the design and development of shell cross-linked nanomaterials with tunable size,<sup>4</sup> shape,<sup>21,22</sup> and core flexibility<sup>23,24</sup> and in the ability to perform chemical modifications selectively within the nano-

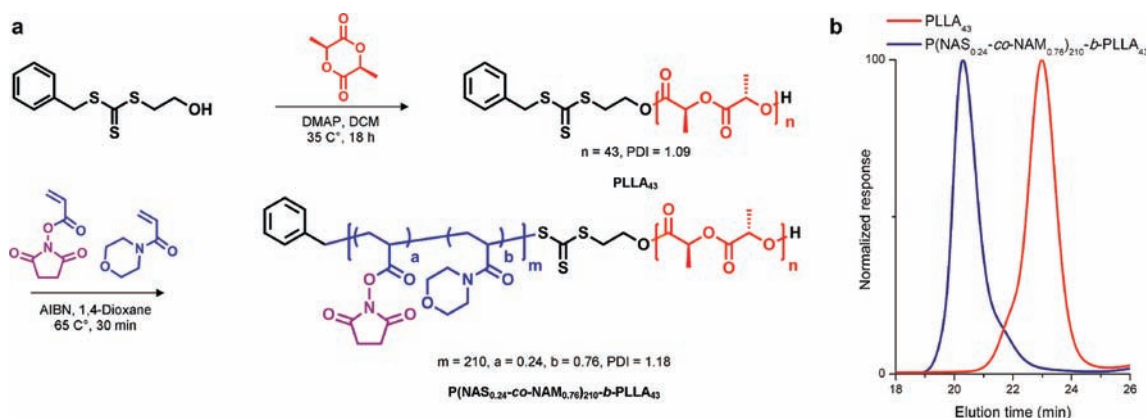
scopic framework.<sup>25,26</sup> These materials are derived from block copolymer micellar assemblies, for which cross-linking performed between reactive units within the shell domain produces shell cross-linked knedel-like (SCK) nanoparticles, providing structural stability to the resulting nanostructures<sup>27</sup> and also gating the trafficking of guest molecules to and from the core.<sup>4,28</sup> Significant efforts have been made to integrate degradability into polymeric nanoparticles by the use of various types of hydrolytically cleavable polymers, such as poly( $\epsilon$ -caprolactone) (PCL), as the hydrophobic core domain of cross-linked<sup>13,15,16</sup> and worm-like<sup>29</sup> micellar assemblies, enzymatically and hydrolytically degradable PLA in PEG-based nanoparticles,<sup>9–12,14</sup> crystallization-driven cylindrical assemblies,<sup>30</sup> and UV-induced thiolene cross-linked nanocapsules<sup>31</sup> as well as in nanosized sugar balls.<sup>32</sup> The selective excavation of the degradable core or cleavage of a single shell–core connection site of some of these materials via environmental triggers has generated hollow nanocages.<sup>15,32–35</sup> Additionally, chromophore-linked degradable cross-linkers have been incorporated into the shell of SCKs for programmed disassembly of nanostructures and controlled release of reporter molecules,<sup>36</sup> with inspiration from Fréchet's explodable micelles.<sup>37</sup>

As an extension to the previous studies focused on incorporating chemical and hydrolytic degradability into

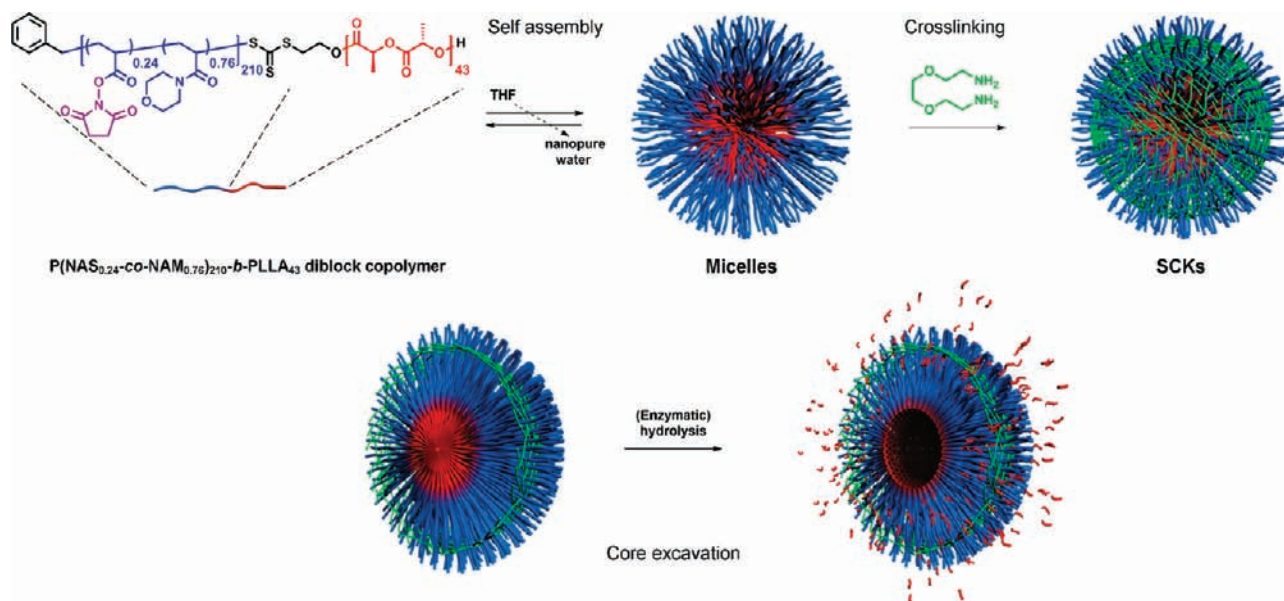
Received: October 11, 2011

Published: December 13, 2011

Scheme 1. (a) Synthesis of PLLA<sub>43</sub> Homopolymer and P(NAS<sub>0.24-co-NAM<sub>0.76</sub></sub>)<sub>210</sub>-*b*-PLLA<sub>43</sub> Diblock Copolymer and (b) Size Exclusion Chromatography Traces of the Homopolymer and Diblock Copolymer Samples, Showing Narrow Molecular Weight Distributions



Scheme 2. Preparation of SCK Nanoparticles by Self Assembly of Amphiphilic Diblock Copolymer P(NAS<sub>0.24-co-NAM<sub>0.76</sub></sub>)<sub>210</sub>-*b*-PLLA<sub>43</sub> Followed by Crosslinking and Production of a Nanocage-Like Structure from Selective Hydrolysis of the PLA Core of the SCK template



nanostructures, this current research integrates degradable PLA and specifically investigates the hydrolytic degradation behaviors of PLA within the core regions of micelles and SCKs, under acid and enzyme catalysis. As the enzymatic cleavage of the PLA core requires the enzyme to be accessible to the core domain, this work also provides information on the permeability of the cross-linked shell.

## RESULTS AND DISCUSSION

Core-degradable SCK nanoparticles were constructed by the supramolecular assembly of a novel amphiphilic diblock copolymer P(NAS<sub>0.24-co-NAM<sub>0.76</sub></sub>)<sub>210</sub>-*b*-PLLA<sub>43</sub>, followed by cross-linking between the *N*-hydroxysuccinimide (NHS)-activated acrylic acid (NAS) functionalities presented within the shell of the nanoparticles by the addition of diamino cross-linkers. Sequential ring-opening polymerization (ROP) and reversible addition–fragmentation chain transfer (RAFT) polymerization were employed to obtain the initial PLLA<sub>43</sub> homopolymer and subsequent P(NAS<sub>0.24-co-NAM<sub>0.76</sub></sub>)<sub>210</sub>-*b*-

PLLA<sub>43</sub> diblock copolymer, each having a narrow molecular weight distribution (Scheme 1). Our design of the amphiphilic diblock copolymer P(NAS<sub>0.24-co-NAM<sub>0.76</sub></sub>)<sub>210</sub>-*b*-PLLA<sub>43</sub> precursor to the micelles and SCKs incorporates a hydrophobic, degradable PLA segment and a P(NAS-*co*-NAM) copolymer segment that provide built-in functionality and hydrophilicity. The choice of P(NAS-*co*-NAM) copolymer as the hydrophilic block was inspired by previous demonstrations of the utility of NAS as a convenient functional handle,<sup>38,39</sup> that also allows in situ synthesis of SCKs by direct cross-linking with elimination of the need for coupling agents.<sup>40</sup>

Block copolymer micelles and SCKs were prepared from P(NAS<sub>0.24-co-NAM<sub>0.76</sub></sub>)<sub>210</sub>-*b*-PLLA<sub>43</sub> by treating the samples to the same conditions throughout the process, with the exception of the addition of a cross-linker. Self-assembly of the diblock copolymer into micelles was afforded by its dissolution in tetrahydrofuran (THF, 1.77 mg/mL), followed by dropwise addition of an equal volume of nanopure water using a syringe pump (7.5 mL/h). The solution was dialyzed against nanopure

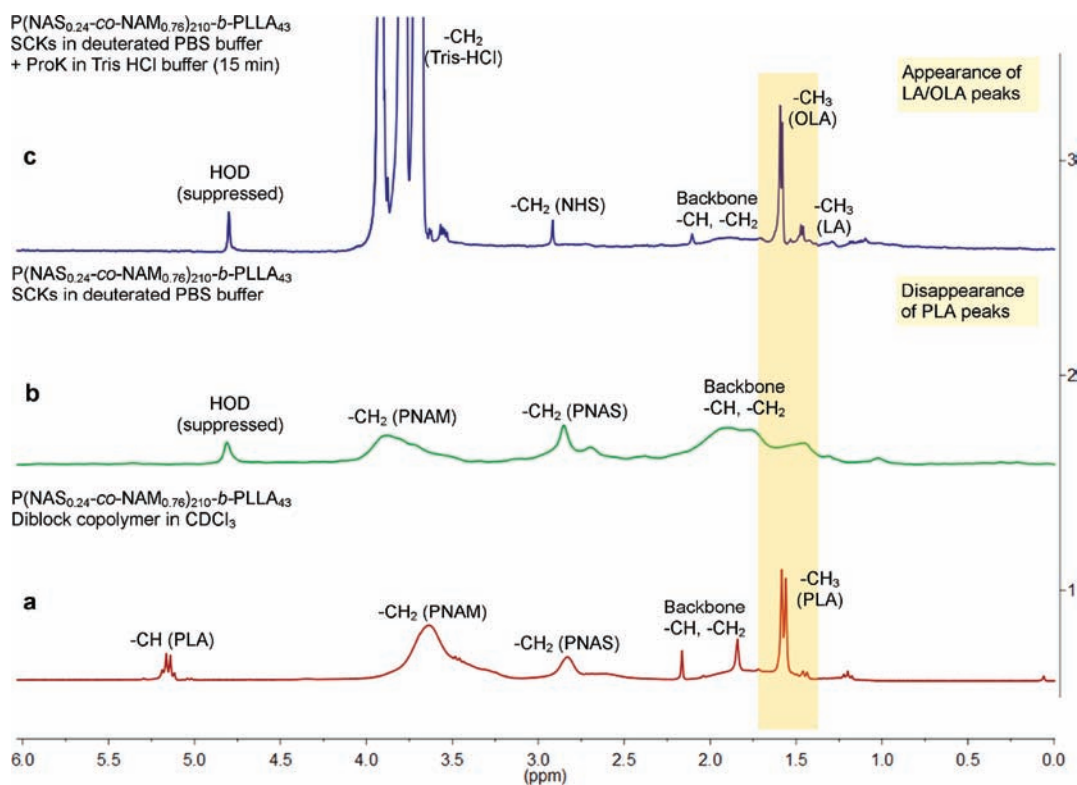


**Figure 1.**  $^1\text{H}$  NMR spectra: (a) diblock copolymer  $\text{P}(\text{NAS}_{0.24}\text{-co-NAM}_{0.76})_{210}\text{-b-PLLA}_{43}$  in  $\text{CDCl}_3$ ; (b) SCKs in deuterated PBS buffer (solvent suppressed) confirming self-assembly of the diblock copolymer by the reduction and/or broadening of the hydrophobic PLA peak intensities; (c) SCKs after 15 min of adding the enzyme (solvent suppressed) confirming degradation of PLA by the appearance of two sets of new OLA/LA peaks.

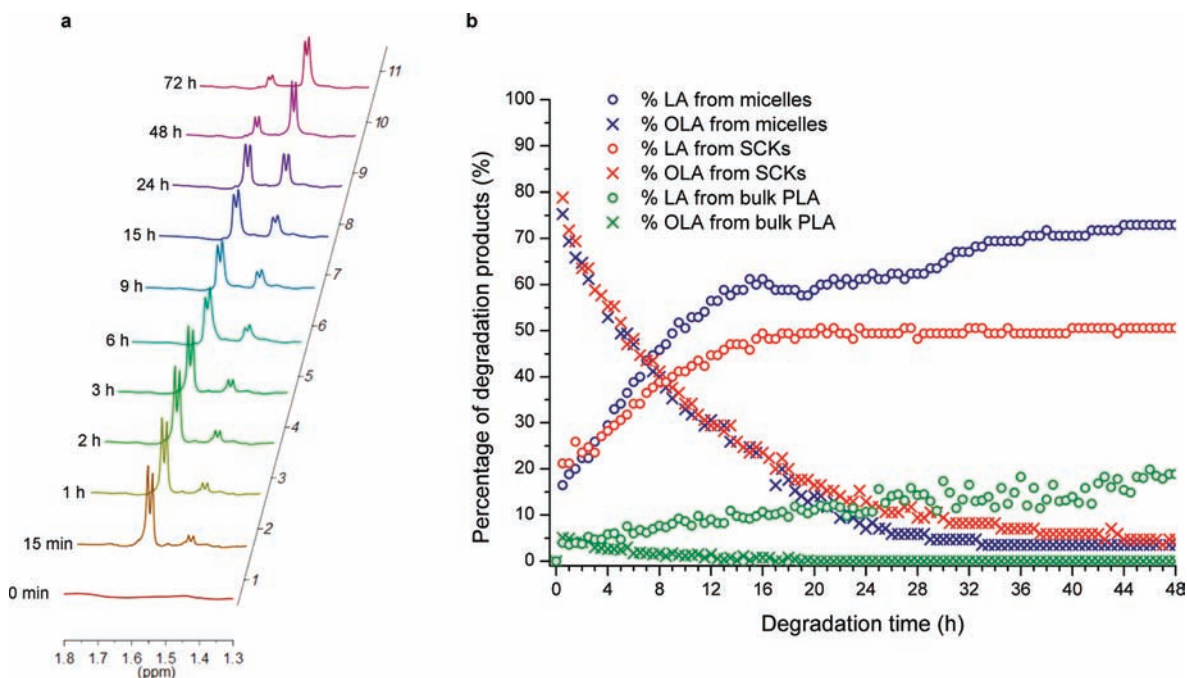


**Figure 2.** (a) Real-time  $^1\text{H}$  NMR spectra of the OLA (1.64–1.56 ppm) and LA (1.48–1.44 ppm) methyl protons for micelles monitored over 3 days following addition of the enzyme. (b) Percent degradation products vs. degradation time plot from integration of OLA or LA peaks from micelles, SCKs, and bulk PLA monitored at 30 min intervals over 48 h of enzyme exposure.

water for 4 days to afford micellar assemblies (0.5 mg/mL). The solution of micelles was divided into two equal volumes, and one of the portions was subjected to a nominal cross-linking density of 20% throughout the shell region by the addition of a diamine cross-linker (2,2'-(ethylenedioxy)bis-

(ethylamine)) to a stirring solution of micelles to yield SCKs. The solution of SCKs was dialyzed against nanopure water for 2 days to remove the NHS byproduct and unreacted cross-linkers. The cross-linking density of 20% refers to the stoichiometry of the amines of the cross-linkers relative to



the initial NAS residues. Additionally, the micellar solution was allowed to undergo dialysis for the same period of time to compensate for any hydrolytic degradation of PNAS and/or PLLA units. The pH values of the two solutions were adjusted to 7–8 by dialysis against 1 mM of PBS buffer containing 0.05% w/v of  $\text{NaN}_3$  for 3 days. Scheme 2 illustrates the preparation of SCK nanoparticles from the polymer precursor and the enzymatic degradation process of the SCKs.

Enzymatic degradation of the PLA core was accomplished by the addition of proteinase K into the two solutions of micelles and SCKs at 37 °C.<sup>41–43</sup> Quantitative analyses of PLA degradation from the nanoparticles were performed by solvent suppression  $^1\text{H}$  NMR spectroscopy. Micelles and SCKs were prepared in deuterated PBS buffer at pH of 7–8, and 0.6 mL of each of the solutions was transferred into NMR tubes for analysis. Assembly of the amphiphilic diblock copolymers into micellar structures in aqueous solution was confirmed by reduction and/or broadening of the NMR peaks corresponding to the hydrophobic PLA segment and observable for the diblock copolymer when solvated in an organic solvent ( $-\text{CH}$ , 5.22–5.10 ppm and  $-\text{CH}_3$ , 1.64–1.52 ppm), due to the inability of the aqueous media to solvate the hydrophobic core region of the nanoparticles (Figure 1a,b). The degradation experiments were conducted by addition of proteinase K (20  $\mu\text{L}$  in tris-HCl buffer, 800 U/mL) into the NMR tubes and collection of spectra at 30 min time intervals for 48 h, maintaining the instrument temperature at 37 °C. To compare the rate of PLA degradation from the cores of the nanostructures vs. bulk PLA, the same kinetics studies were also performed on the PLA homopolymer, as a thin film within an NMR tube.

Real-time monitoring of the enzymatic degradation was accomplished by observing the methyl protons of oligo(lactic acid) (OLA) and lactic acid (LA) ranging from 1.64 to 1.44 ppm in deuterated buffer, in comparison to an external chloroform reference. Interestingly, within 15 min of adding the enzyme, two new sets of peaks were apparent at 1.64–1.56 and 1.48–1.44 ppm (Figure 1c), in which the intensity of the peaks corresponding to the methyl protons from LA (1.48–1.44 ppm) continued to increase at the expense of the peaks corresponding to OLA (1.64–1.56 ppm). Figure 2a represents the real-time  $^1\text{H}$  NMR spectra of the OLA/LA methyl protons for micelles monitored for 3 days following addition of the enzyme.

To confirm that the degradation of PLA was facilitated by the enzyme and not by noncatalyzed hydrolysis, control experiments were performed. In the absence of the enzyme, the NMR spectra did not show any OLA or LA proton signals within 48 h of monitoring (data not shown). Also, as an identification and confirmation of the production of LA from PLA, at the end of the degradation experiment, one of the NMR tubes containing degraded PLA was spiked with LA externally and an increase in the peak intensity at 1.48–1.44 ppm was observed.

Having demonstrated that PLA degradation occurred in the presence of the enzyme, our primary goal of the NMR studies was to quantify and compare the degradation behavior of the micelles as opposed to the cross-linked material, in order to determine if the cross-linking provided a barrier to the enzyme to permeate through the shell. We were also interested in the rates of hydrolysis for the nanomaterials vs bulk PLA. The hydrolysis rates of PLA were measured by comparing the relative amounts of LA and OLA generated from micelles and SCKs to the 100% PLA determined by lyophilization of an

equal volume of micelles followed by analysis in  $d_6$ -DMSO, a solvent for the entire diblock copolymer. For the bulk sample, the total amount of PLA was known, due to the use of a stock solution for the sample preparation. During the quantification process, the same external reference of chloroform, in the form of a sealed capillary tube, was used in all the NMR tubes for accurate integration purposes. As illustrated in Figure 2b, which summarizes the kinetic analysis of the degradation processes determined from NMR spectroscopy, ca. 80% of the total OLA was observable for the micelles and SCKs within 15 min, whereas continued degradative conversion to LA occurred more rapidly for the micelles than for the SCKs. LA production from SCKs began to plateau after ca. 15 h of exposure to enzyme, reaching a maximum percent degradation of approximately 50% of the PLA core. However, the LA generation from micelles continued to increase to about 70% through 48 h of exposure to the enzyme. In comparison, the bulk thin film PLA underwent only <20% LA generation over 48 h incubation with the enzyme solution and gave an OLA signal that reached only ca. 5%. These results confirm the ability of the enzyme to gain access to the PLA, when packaged within a micelle or SCK core and when fully exposed. Given the dimensions of the enzyme (2–3 nm), it is expected that migration through the SCK shell requires some degree of cleavage of the amide cross-linkers, as migration of macromolecules through SCK shells has been shown to be limited by the cross-links.<sup>44</sup> It is intriguing that neither the OLA nor the LA proton signals was observed until the addition of the enzyme was performed, yet it remains uncertain whether the OLA signal is due to free oligomers in solution or to mobile lactic acid repeat units that remained connected to the PLA of the nanostructures or thin film. The differences observed for continued breakdown into LA for the micelles vs SCKs suggest that the OLA remained as part of the nanostructures. The cross-links within the shells of the SCKs were shown to behave as gates, limiting migration of the enzyme through the shell to gain access to the PLA/OLA and/or mobility of the PLA/OLA to the SCK surface to expose some portion of the PLA chain segments, initially and upon potential reorganization events as the degradation proceeded. The similar kinetics for the initial OLA production for both the micelles and SCKs suggest that the cross-linked shell posed no barrier to the enzyme and merely reduced the rate of conversion of OLA to LA.

The relatively rapid enzymatic degradation kinetics of the PLA core, especially within 15 min of adding the enzyme may be attributed to the possible interactions between the negatively charged surface of the nanoparticles and the positively charged enzyme at the physiological pH conditions applied. Partial hydrolysis of the NAS units in the shell of the nanoparticles gave rise to an anionic shell ( $\zeta$  potential:  $-35 \pm 2$  and  $-48 \pm 3$  mV for freshly prepared micelles and SCKs, respectively, at pH of 7–8) that could readily attract the positively charged proteinase K (isoelectric point 8.9)<sup>45</sup> to the nanoconstructs, following rapid degradation of the core material. A control study using lipase (isoelectric point 4.9), which should be electrostatically repelled from the SCKs observed no PLA degradation.

Because proteinase K is capable of cleaving amide-based cross-links within the SCK shells, in addition to the observed rapid degradation of the PLA core, we investigated the integrity of the nanoparticle upon core excavation. In order to thoroughly evaluate and compare the fate of the nanoparticles, especially the stability of micelles compared to SCKs upon

hydrolysis of PLA, a series of analytical tools, including dynamic light scattering (DLS), transmission electron microscopy (TEM), and atomic force microscopy (AFM), was utilized.

DLS studies provided insight into the dimensional changes in the hydrodynamic diameters of the nanoparticles upon core excavation. It was observed that upon hydrolysis of the PLA segment, the resulting hydrophilic nanocage-like structures underwent swelling, due to the diffusion of water into the core region, increasing progressively as the hydrophobic components were eliminated. The swelling process was monitored for both micelles and SCKs upon hydrolytic as well as enzymatic degradation of PLA. As shown in Figure 3, the initial number-

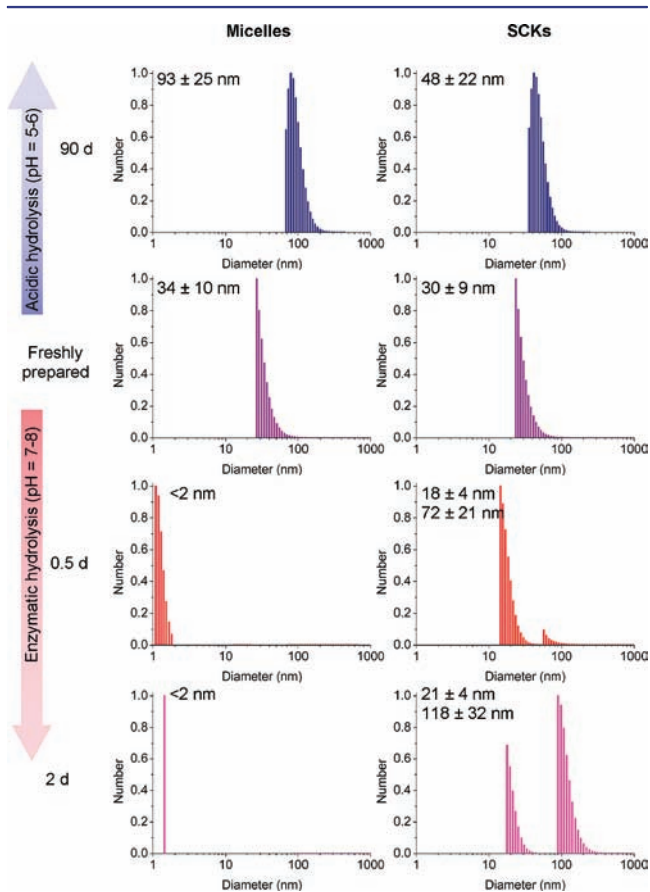


**Figure 3.** Examination of changes in hydrodynamic diameters by dynamic light scattering for micelles and SCKs as a function of acidic and enzymatic hydrolysis times.

average hydrodynamic diameters ( $D_{h(n)}$ ) of micelles and SCKs were  $34 \pm 10$  and  $30 \pm 9$  nm, respectively. For micelles, while hydrolytic degradation for 3 months in nanopure water at pH of 5–6 expanded the hydrodynamic diameter to  $93 \pm 25$  nm, after 12 h of enzymatic degradation micelles were no longer detectable from DLS, indicating complete disassembly of the particles. The significant increase in  $D_h$  under hydrolytic conditions is expected to be the result of micellar reorganization events, including polymer chain exchange and micelle aggregation, as the hydrophobic chain segment lengths decrease over time and hydrophilic surface chains are released from the micelle assemblies. Although the cross-linked analog showed a similar trend for expansion upon hydrolytic degradation over the same period of 3 months, their  $D_h$  increased only to  $48 \pm 22$  nm, suggesting shell expansion in the absence of additional micellar reorganization and

aggregation. Also in contrast to the micelles, 12 h of enzymatic degradation of SCKs did not result in complete disassembly but rather showed a dual distribution in the hydrodynamic diameter to  $18 \pm 4$  and  $72 \pm 21$  nm and further expansion to  $21 \pm 4$  and  $118 \pm 32$  nm after 48 h of enzymatic incubation.

To further assess the dimensional changes observed from DLS, the nanoparticles were observed under TEM. Freshly prepared nanoparticles were well-defined and uniform in size as shown in Figure 4, with average core diameters of  $7 \pm 1$  and  $9$

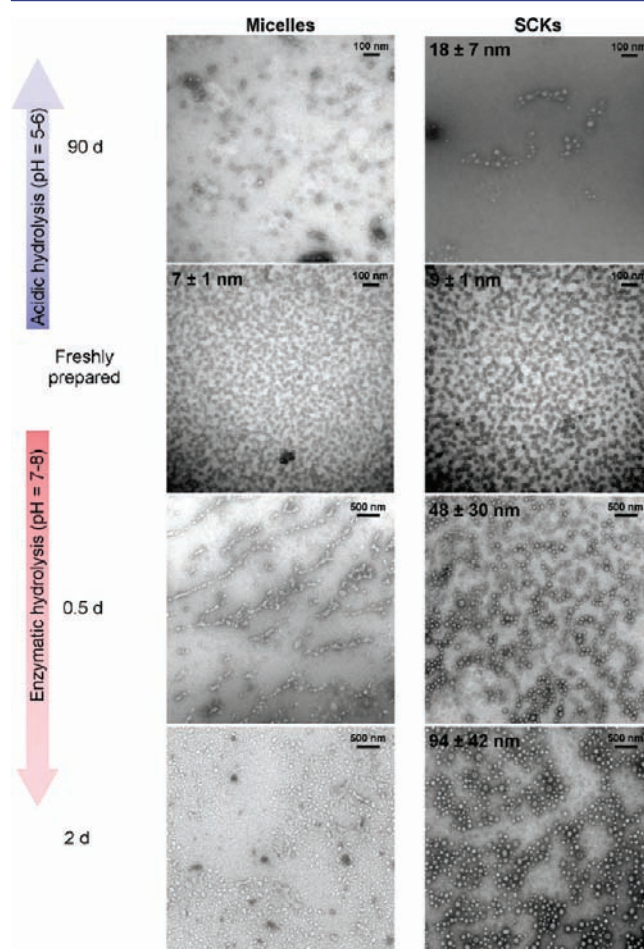


**Figure 4.** Examination of changes in average core diameters in the dry state by transmission electron microscopy for micelles and SCKs as a function of acidic and enzymatic hydrolysis times.

$\pm 1$  nm for micelles and SCKs, respectively. After 90 days of hydrolysis in water, micelles showed ill-defined nonspherical particles in the dry state, while SCKs showed approximately 50% increases in the core diameters, expanding to  $18 \pm 7$  nm. These results were consistent with the increases in the hydrodynamic diameters upon partial hydrolysis of the PLA core observed by DLS measurements. Interestingly, enzymatically hydrolyzed micelles, which showed from NMR ca. 55% of the PLA cores degraded within 12 h, appeared as ill-defined polymer aggregates under TEM imaging. In contrast to micelles, SCKs remained robust and appeared as hollowed-out nanocage-like structures with a broad distribution of core diameters ( $48 \pm 30$  nm) in agreement with DLS measurements. After 48 h of enzyme treatment, completely degraded micellar structures looked similar to the 12 h time point under TEM, while SCKs showed further expansion to  $94 \pm 42$  nm.

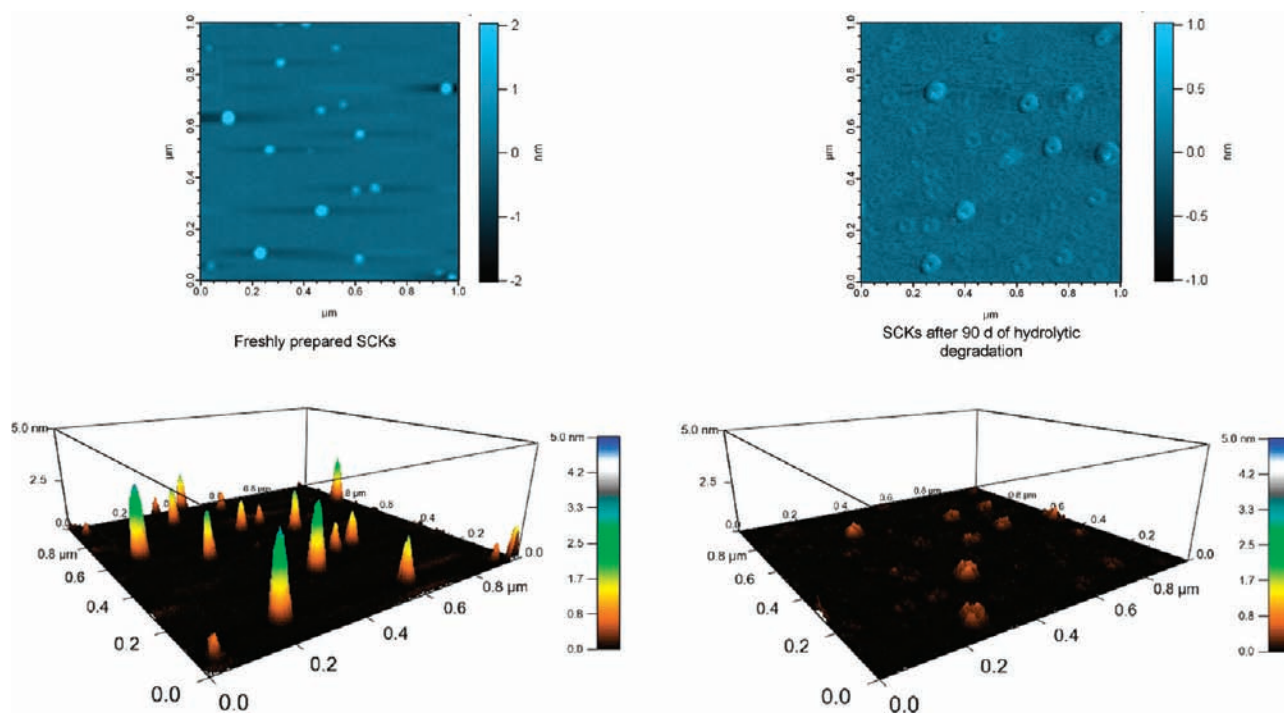


**Figure 5.** Tapping-mode AFM images of freshly prepared SCKs and hydrolytically degraded SCKs, showing collapse of the nanocage-like structures on the mica substrate upon core excavation.

In our previous work, it has been observed from AFM that SCK nanoparticles composed of soft core material undergo a flattening process upon adsorption on to the mica substrate, resulting in a decreased particle height and increased diameter compared to the hydrodynamic diameters observed from DLS.<sup>46–48</sup> As illustrated in Figure 5, AFM images revealed the conversion of SCK nanoparticles to hollowed nanocages (which appear as donut-like structures after collapse onto the mica substrate) upon hydrolytic degradation of the PLA core for 3 months, with a reduction of the particle heights (from  $3 \pm 1$  to  $<1$  nm, before and after hydrolytic core degradation, respectively) and a substantial increase in the average particle width (from  $38 \pm 10$  to  $88 \pm 12$  nm, before and after hydrolytic core degradation, respectively). Even though the DLS data indicated further expansion of the SCKs upon enzymatic degradation, particles were not detectable from AFM after 2 days excavation of the core.

As a measure of the reduction of hydrophobicity within the SCKs upon removal of the PLA region, a reporter molecule Nile red was encapsulated into the nanoparticles. Nile red is a solvatochromic dye that fluoresces intensely under hydrophobic environments but displays weak emission in aqueous media.<sup>49</sup> With an excess amount of Nile red, 35 equal volumes of freshly prepared SCKs, enzymatically degraded SCKs (2 days), and hydrolytically degraded SCKs (90 days) were incubated. The dye was dispersed into aqueous solutions of the nanostructures from THF and allowed to stir overnight. The solutions were sparged with nitrogen to remove THF, and residual dye was removed by filtration through a  $0.45 \mu\text{m}$  Teflon membrane to afford a bright magenta solution of freshly prepared SCKs, a light magenta solution of partially hydrolyzed SCKs, and a pale magenta-to-colorless solution of enzymatically degraded SCKs. Fluorescence measurements were conducted by collecting emission spectra ( $\lambda_{\text{ex}} = 535 \text{ nm}$ ) of the three solutions (Figure 6). The profound loss in fluorescence intensity of the Nile red

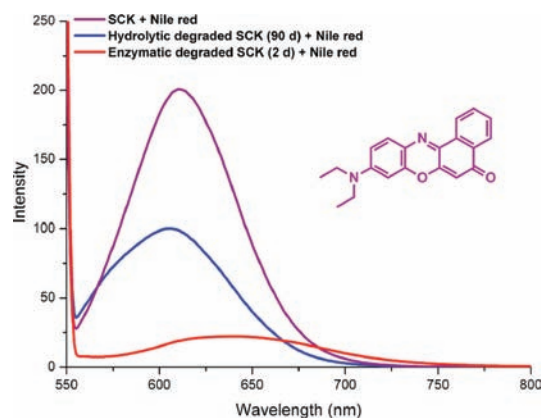


**Figure 6.** Fluorescence intensity when reporter molecule Nile red is encapsulated into SCKs vs hydrolyzed SCKs.

loaded into the solutions that had undergone degradation confirmed the loss of hydrophobicity upon (enzymatic) hydrolysis of the PLA core of the SCKs.

## CONCLUSIONS

In summary, we have reported fundamental advances in the synthetic methodologies for the preparation of hydrolytically degradable, functionalizable nanoparticles, together with rigorous characterization of their degradation properties. Specifically, we have demonstrated enzyme-triggered selective excavation of the polyester-based core of block copolymer micelle assemblies and their shell cross-linked nanoparticle analogs. The rates of hydrolysis of the PLA from the cores of the block copolymer micelles and SCKs were significantly greater than for bulk PLA. Although it is not surprising that having the PLA dispersed in nanoscopic form throughout the solutions resulted in greater ability of the enzymes to access the PLA, rapid migration of the enzyme through the cross-linked



shell layer is curious and worth further investigation, to determine whether the mechanism is by diffusion only or is also facilitated by cleavage of some portion of the cross-links. In contrast to their noncross-linked analogs, which undergo complete disassembly upon loss of their hydrophobic moieties, SCK nanoparticles maintain their nanoparticulate integrity even in the absence of its amphiphilicity. Therefore, any cleavage of the amide-based cross-links is not detrimental to the resulting nanocage framework. Studies are being continued to explore the effect of varying shell cross-linking densities on the core degradation properties of the SCKs. Additionally, loading of active therapeutics into the PLA-based SCKs and the release kinetics of the guest molecules as a function of core degradation are being evaluated and will be reported in the near future.

## ■ ASSOCIATED CONTENT

### ■ Supporting Information

Detailed experimental procedures including polymer synthesis, nanoparticle preparation, degradation conditions, and characterization. This material is available free of charge via the Internet at <http://pubs.acs.org>.

## ■ AUTHOR INFORMATION

### Corresponding Author

wooley@chem.tamu.edu

### Present Address

<sup>§</sup>Massachusetts General Hospital and Harvard Medical School, Boston, Massachusetts 02129, United States.

## ■ ACKNOWLEDGMENTS

We gratefully acknowledge financial support from the National Heart Lung and Blood Institute of the National Institutes of Health as a Program of Excellence in Nanotechnology (HHSN268201000046C) and Covidien, Inc. The Welch Foundation is gratefully acknowledged for support through the W. T. Doherty-Welch Chair in Chemistry, grant no. A-0001. Dr. A. d'Avignon and Dr. K. P. Sarathy of the NMR facilities at Washington University in St. Louis and Texas A&M University, respectively, are gratefully acknowledged for assistance with NMR experiments. The authors would also like to thank Dr. Krishnamurthy Shanmuganandamurthy for initiating this research work, Shiyi Zhang and Dr. Jiong Zou for discussions and support, and Hasitha Samarajeewa for creating the Autodesk 3ds Max images.

## ■ REFERENCES

- (1) Schmitt, E. E.; Polistina, R. A. Surgical sutures. U.S. Patent 3,297,033, January 10, 1967.
- (2) Hoffman, A. S. *J. Controlled Release* **2008**, *132*, 153–163.
- (3) Boswell, G.; Scribner, R. Polyactide-drug mixtures. U.S. Patent 3,773,919, November 20, 1973.
- (4) Lin, L. Y.; Lee, N. S.; Zhu, J. H.; Nystrom, A. M.; Pochan, D. J.; Dorshow, R. B.; Wooley, K. L. *J. Controlled Release* **2011**, *152*, 37–48.
- (5) Broaders, K. E.; Pastine, S. J.; Grandhe, S.; Frechet, J. M. J. *Chem. Commun.* **2011**, *47*, 665–667.
- (6) Lendlein, A.; Jiang, H. Y.; Junger, O.; Langer, R. *Nature* **2005**, *434*, 879–882.
- (7) Lendlein, A.; Langer, R. *Science* **2002**, *296*, 1673–1676.
- (8) Peer, D.; Karp, J. M.; Hong, S.; Farokhzad, O. C.; Margalit, R.; Langer, R. *Nat. Nanotechnol.* **2007**, *2*, 751–760.
- (9) Yamamoto, Y.; Yasugi, K.; Harada, A.; Nagasaki, Y.; Kataoka, K. *J. Controlled Release* **2002**, *82*, 359–371.
- (10) Iijima, M.; Nagasaki, Y.; Okada, T.; Kato, M.; Kataoka, K. *Macromolecules* **1999**, *32*, 1140–1146.

- (11) Rijcken, C. J.; Snel, C. J.; Schiffelers, R. M.; van Nostrum, C. F.; Hennink, W. E. *Biomaterials* **2007**, *28*, 5581–5593.
- (12) Sun, J.; Chen, X. S.; Lu, T. C.; Liu, S.; Tian, H. Y.; Guo, Z. P.; Jing, X. B. *Langmuir* **2008**, *24*, 10099–100106.
- (13) Van Horn, B. A.; Wooley, K. L. *Macromolecules* **2007**, *40*, 1480–1488.
- (14) Kang, N.; Perron, M. E.; Prud'homme, R. E.; Zhang, Y. B.; Gaucher, G.; Leroux, J. C. *Nano Lett.* **2005**, *5*, 315–319.
- (15) Zhang, Q.; Remsen, E. E.; Wooley, K. L. *J. Am. Chem. Soc.* **2000**, *122*, 3642–3651.
- (16) Li, Y. L.; Zhu, L.; Liu, Z. Z.; Cheng, R.; Meng, F. H.; Cui, J. H.; Ji, S. J.; Zhong, Z. Y. *Angew. Chem.-Int. Ed.* **2009**, *48*, 9914–9918.
- (17) Tan, J. P. K.; Kim, S. H.; Nederberg, F.; Appel, E. A.; Waymouth, R. M.; Zhang, Y.; Hedrick, J. L.; Yang, Y. Y. *Small* **2009**, *5*, 1504–1507.
- (18) Kim, S. H.; Tan, J. P. K.; Nederberg, F.; Fukushima, K.; Yang, Y. Y.; Waymouth, R. M.; Hedrick, J. L. *Macromolecules* **2009**, *42*, 25–29.
- (19) Gref, R.; Minamitake, Y.; Peracchia, M. T.; Trubetskoy, V.; Torchilin, V.; Langer, R. *Science* **1994**, *263*, 1600–1603.
- (20) Karnik, R.; Valencia, P. M.; Hanewich-Hollatz, M. H.; Gao, W. W.; Karim, F.; Langer, R.; Farokhzad, O. C. *Biomaterials* **2011**, *32*, 6226–6233.
- (21) Pochan, D. J.; Chen, Z. Y.; Cui, H. G.; Hales, K.; Qi, K.; Wooley, K. L. *Science* **2004**, *306*, 94–97.
- (22) Lee, N. S.; Sun, G.; Lin, L. Y.; Neumann, W. L.; Freskos, J. N.; Karwa, A.; Shieh, J. J.; Dorshow, R. B.; Wooley, K. L. *J. Mater. Chem.* **2011**, *21*, 14193–14202.
- (23) Zhang, Q.; Wang, M.; Wooley, K. L. *Curr. Org. Chem.* **2005**, *9*, 1053–1066.
- (24) Nystrom, A. M.; Wooley, K. L. *Soft Matter* **2008**, *4*, 849–858.
- (25) Sun, G.; Hagooly, A.; Xu, J.; Nystrom, A. M.; Li, Z. C.; Rossin, R.; Moore, D. A.; Welch, M. J.; Wooley, K. L. *Biomacromolecules* **2008**, *9*, 1997–2006.
- (26) Zhang, S.; Li, Z.; Samarajeewa, S.; Sun, G. R.; Yang, C.; Wooley, K. L. *J. Am. Chem. Soc.* **2011**, *133*, 11046–11049.
- (27) Sorrells, J. L.; Shrestha, R.; Neumann, W. L.; Wooley, K. L. *J. Mater. Chem.* **2011**, *21*, 8983–8986.
- (28) Lee, N. S.; Lin, L. Y.; Neumann, W. L.; Freskos, J. N.; Karwa, A.; Shieh, J. J.; Dorshow, R. B.; Wooley, K. L. *Small* **2011**, *7*, 1998–2003.
- (29) Geng, Y.; Discher, D. E. *J. Am. Chem. Soc.* **2005**, *127*, 12780–12781.
- (30) Petzetakis, N.; Dove, A. P.; O'Reilly, R. K. *Chem. Sci.* **2011**, *2*, 955–960.
- (31) Zou, J.; Hew, C. C.; Themistou, E.; Li, Y.; Chen, C.-K.; Alexandridis, P.; Cheng, C. *Adv. Mater.* **2011**, *23*, 4274–4277.
- (32) Ting, S. R. S.; Gregory, A. M.; Stenzel, M. H. *Biomacromolecules* **2009**, *10*, 342–352.
- (33) Ievins, A. D.; Moughton, A. O.; O'Reilly, R. K. *Macromolecules* **2008**, *41*, 3571–3578.
- (34) Moughton, A. O.; Stubenrauch, K.; O'Reilly, R. K. *Soft Matter* **2009**, *5*, 2361–2370.
- (35) Zhang, Y.; Jiang, M.; Zhao, J.; Wang, Z.; Dou, H.; Chen, D. *Langmuir* **2005**, *21*, 1531–1538.
- (36) Li, Y. L.; Du, W. J.; Sun, G. R.; Wooley, K. L. *Macromolecules* **2008**, *41*, 6605–6607.
- (37) Gillies, E. R.; Frechet, J. M. J. *Chem. Commun.* **2003**, 1640–1641.
- (38) Li, Y. T.; Lokitz, B. S.; McCormick, C. L. *Macromolecules* **2006**, *39*, 81–89.
- (39) Handke, N.; Trimaille, T.; Luciani, E.; Rollet, M.; Delair, T.; Verrier, B.; Bertin, D.; Gimes, D. *J. Polym. Sci., Part A: Polym. Chem.* **2011**, *49*, 1341–1350.
- (40) Li, Y. L.; Akiba, I.; Harrison, S.; Wooley, K. L. *Adv. Funct. Mater.* **2008**, *18*, 551–559.
- (41) Williams, D. F. *Eng. Med.* **1981**, *10*, 5.
- (42) Xiong, X. Y.; Tam, K. C.; Gan, L. H. *J. Controlled Release* **2005**, *108*, 263.
- (43) MacDonald, R. T.; McCarthy, S. P.; Gross, R. A. *Macromolecules* **1996**, *29*, 7356.

- (44) Murthy, K. S.; Ma, Q.; Clark, C. G. Jr.; Remsen, E. E.; Wooley, K. L. *Chem. Commun.* **2001**, 773–774.
- (45) Ebeling, W.; Hennrich, N.; Klockow, M.; Metz, H.; Orth, H. D.; Lang, H. *Eur. J. Biochem.* **1974**, *47*, 91–97.
- (46) Turner, J. L.; Wooley, K. L. *Nano Lett.* **2004**, *4*, 683–688.
- (47) Huang, H. Y.; Remsen, E. E.; Kowalewski, T.; Wooley, K. L. *J. Am. Chem. Soc.* **1999**, *121*, 3805–3806.
- (48) Ma, Q. G.; Remsen, E. E.; Kowalewski, T.; Schaefer, J.; Wooley, K. L. *Nano Lett.* **2001**, *1*, 651–655.
- (49) Greenspan, P.; Mayer, E. P.; Fowler, S. D. *J. Cell Biol.* **1985**, *100*, 965–973.